A study of crown development mechanisms using a shoot-based tree model and segmented terrestrial laser scanning data

Sievänen, Risto

2018-09-01

Sievänen , R , Raumonen , P , Perttunen , J , Nikinmaa , E H & Kaitaniemi , P J 2018 , ' A study of crown development mechanisms using a shoot-based tree model and segmented terrestrial laser scanning data ' , Annals of Botany , vol. 122 , no. 3 , pp. 423-434 . https://doi.org/10.1093/aob/mcy08

http://hdl.handle.net/10138/308580
https://doi.org/10.1093/aob/mcy082

Original article

A study into crown development mechanisms using a shoot-based tree model and segmented TLS data

Risto Sievänen[1*], Pasi Raumonen[2], Jari Perttunen[1], Eero Nikinmaa[3], and Pekka Kaitaniemi[4]

(1) Natural Resources Institute Finland, Latokartanontie 9, 00790 Helsinki, Finland,

(2) Laboratory of Mathematics, Tampere University of Technology, P.O. Box 553, 33101 Tampere

(3) Department of Forest Sciences, University of Helsinki, Latokartanonkaari 7, (P.O. BOX 27), 00014 University of Helsinki, Finland,

(4) Hyytiälä Forestry Field Station University of Helsinki, Hyytiäläntie 124, 35500 Korkeakoski, Finland

*Corresponding author: risto.sievanen@luke.fi

ABSTRACT

•**Background and Aims** The functional structural plant models (FSPMs) allow simulation of tree crown development as the sum of modular (e.g. shoot level) responses triggered by the local environmental conditions. The actual process of space filling by the crowns can be studied. Although the FSPM simulations are at organ scale, the data for their validation have usually been at more aggregated levels (whole crown or whole tree). Measurements made by

terrestrial laser scanning (TLS) that have been segmented to elementary units (internodes) offer a phenotyping tool to validate the FSPM predictions at comparable levels to their detail. We demonstrate in this contribution testing different formulations of crown development of Scots pine trees in LIGNUM model using segmented TLS data.

•**Methods** We made TLS measurements from four sample trees growing in a forest on a relatively poor soil from a sapling size to a mature stage. The TLS data were segmented into internodes. The segmentation also produced information whether needles were present in the internode. We applied different formulations of crown development (flushing of buds and length growth of new internodes) in LIGNUM. We optimized the parameter values of each formulation using genetic algorithms to observe the best fit of LIGNUM simulations to the measured trees. The fitness function in the estimation combined both tree level characteristics (e.g. tree height and crown length) as well as measures of crown shape (e.g. spatial distribution of needle area).

•**Key Results** Comparison of different formulations against the data indicates that Extended Borchert-Honda model for shoot elongation works best within LIGNUM. Control of growth by local density in the crown was important for all shoot elongation formulations. Modifying the number of lateral buds as a function of local density in crown was the best way to accomplish density control.

Conclusions It was demonstrated how segmented TLS data can be used in the context of a shoot-based model to select model components.

Keywords: Functional-structural model, forest stand, Scots pine, terrestrial laser scanning

INTRODUCTION

The three principal interacting processes involved in the growth of a tree, and thus stand development, are (Ford and Sorrensen, 1992): (1) resource capture as a response to the immediate environment and leading to tree growth, (2) allocation of growth to the development of the 3D structure of the tree and, consequently, (3) modification of the immediate environment, described as a three-dimensional distribution of the resource flux. The stand dynamics result from the interplay of these processes, and is primarily reflected in crown development: if the tree can lift its crown to a position that affords sufficient light in comparison to its competitors, then it will survive in the stand, otherwise it will become suppressed and is liable to die. These growth processes have been modeled in the functional structural plant models (FSPMs; Godin and Sinoquet 2005) and other modular plant models in various ways. They treat trees as modular organisms in the sense of Franco (1986): "The growth and form of a modular organism is determined by the rigid rules of iteration (branching) and the differential response of each growing point to the local conditions around it. The degree of response of each individual module is itself dependent on the degree of physiological integration of the whole organism."

In those models, thus, individual buds are created, they develop to growth units that carry foliage and buds or die or become dormant if their local conditions are not favorable. This process has been modeled at many levels of detail and abstraction. Constraints and strategies of arborescent plant growth have been studied at abstract level e.g. by Takenaka (1994), Sterck and Schieving (2007), Palubicki et al. (2009) and Palubicki (2013). An example of a generic model that can be adjusted to specific conditions is GreenLab (e.g. Cournede et al. 2008). It applies a system of equations based on resource acquisition, distribution of resources between

sources and sinks and morphological development relying on botanical rules. It has been applied for example to beech (Letort et al. 2008) and Mongolian pine (Wang et al 2012). There are many models that have been constructed specifically to one species. ECOPHYS for poplar (Host et al. 2008), L-PEACH (Da Silva et al. 2014) for peach and MAppleT (Costes et al. 2008) for apple trees are examples of such models.

Detailed, precise, 3D representations of individual trees are necessary for an accurate assessment of any of the above-mentioned models. The laborious destructive measurements used so far have limited the extent of validation studies severely. Terrestrial laser scanning (TLS) methods have developed quickly. They now provide some superior advantages compared to the traditional and partly manual methods to measure trees. TLS methods allow us to measure non-destructively and fast 3D characteristics of tree crowns (e.g. Raumonen et al 2013, Gatziolis et al. 2015 and Potapov et al. 2016) that were earlier very time consuming to assess. TLS's are providing conveniently detailed data of crown structures: precise, detailed 3D representations of individual trees. TLS data are finding their way to fitting detailed tree models (e.g. Beyer et al. 2017a, 2017b).

In this paper, we make use of TLS data of trees and demonstrate their use to study different rules of development that have been proposed to govern structural organization of tree crowns. As rules of development we tested some variants of competition between buds and branches for light and space (Perttunen et al 1996, Palubicki et al. 2009), as well as growth controlled by the vigor index (Nikinmaa et al. 2003). The rules of development were implemented in the shoot-based tree growth model LIGNUM (Perttunen et al 1996, Sievänen et al. 2008). We compared the rules of development by observing how well LIGNUM equipped with the particular rule matched the actual data of growth of Scots pine trees obtained by TLS. For this

used an optimization method (Genetic algorithm) but did not aim at parameter estimation, only finding general differences between rules of development.

MATERIAL AND METHODS

THE APPROACH TO TESTING

We tested the agreement with data from Scots pine trees of rules of crown development that were implemented in LIGNUM model (Perttunen et al. 1996, Sievänen et al. 2008), Fig. 1. The agreement was measured with the aid of fit statistics (loss function). The data comprised TLS measurements of four trees at ages 8, 16, 25 and 33 years.

We compared alternative formulations for model components that were responsible for shoot elongation and production of new buds within crown. The parameter values of those model components were optimized for best agreement with the TLS data using genetic algorithm (Scrucca 2013). Because our focus was on the comparison of alternative rules of development we were not interested in the particular values of parameters that produced the best agreement with the data. Instead, the optimization served just to find the full potential of the rule of development. Parameter estimation would require an identifiability analysis to find out if model parameters are determined by the available TLS data. Such attempt warrants a separate study with a larger sample.

All the other crown processes included in LIGNUM were left intact and were implemented as in Sievänen et al. (2008). Altogether, we tested model components from three categories: shoot

elongation, effect of local shoot density in crown and height preference of growth allocation. This produced 18 different combinations model components, which were fitted to the data (Fig. 1). The combinations are detailed in Supplementary material2. In the fitting, many functions involved in tested model components were implemented as piecewise linear curves parameterized to follow the general shape of the model functions (cf. Fig. 1). The fit statistics, that is, loss function combined both tree and shoot level characteristics of trees (Eq. 12). A genetic algorithm was used to minimize the loss function with respect of parameter values that were specific for each combination of model components. After reaching the best agreement with the data, the ranking of alternative model formulations and combinations was compared on the basis of value of the loss function.

TARGET TREES BY TLS

We created a pseudo growth sequence of Scots pine trees by scanning point clouds of four Scots pine trees at different ages of even aged stands growing on dryish upland sites (VT in the Finnish forest classification system; Cajander 1949) near to each other in the vicinity of Helsinki. The stands were even-aged pure Scots pine stands. The ages of forests (and thus the trees) were 8, 16, 25 and 33 years, and approximate densities 6600, 3000, 1660, and 1000 trees per hectar. The mean heights of forest stands (from youngest to oldest) were 2.5 m, 6.7 m, 10.7 m and 13.9 m. The sample trees were selected sufficiently close (subjective assessment) to average tree. The heights of scanned trees were 2.6 m, 7.2 m, 12.0 m, and 13.6 m (Fig. 9). The forests had been managed according to common forestry practices. The scanned trees can therefore be considered to present a tree in different phases of pine forest growth.

The sample trees were scanned from three locations around the tree at distances 3-5 m with Riegl VZ-400 scanner with vertical and horizontal point density 40 mdeg. The scans were co-registered; the point clouds contained 578308, 7827896, 1533189 and 5024371 points (from youngest to oldest tree). Each point cloud was first segmented into individual branches using the segmentation method presented in (Raumonen et al. 2013, Calders et al. 2015). The segmentation process randomly partitions the point cloud into small subsets whose diameters are about few centimetres and whose neighbours are defined. Starting from the bottom of the point cloud, which is the base of the stem, we use surface growing with these subsets step-by-step adding new layer of neighbours. At each step, bifurcation points are identified by checking local connectivity of the top few layers of the subsets. After the bifurcation or branching points are determined, the final segments (branches) are defined in the increasing branching order by making each segment to reach as far as possible from its base. The result is a division of the point cloud into segments (branches) that do not have any bifurcations along them and whose volume and surface can be next modelled with consecutive cylinders.

Next each branch was modelled with a number of cylinders whose relative length (length/radius) was about a user-given constant. The cylinders were fitted to data using least squares method with the aim of reconstructing the woody surface and volume. We observed that the cylinders fitted to regions with needles had a tendency to be too large in comparison to what can be expected on the basis of tapering of branches. We used this trait of segmentation to asses if there are needles in a branch. To recognize if a cylinder was too thick, we employed a loose parabola taper correction that enforces a generally decreasing taper and gives the local maximum and minimum radius for the cylinders. The parabola taper is defined based on the cylinders fitted in the first three quarters of the branch and setting the radius to 2.5 mm at the

tip of the branch. More details of the taper correction can be found in (Calders et al. 2015). Now, if the corrected radius was at least 30% lower than the fitted radius, then we took that as an indication of existence of needles. If a branch contained cylinders with needles, then we also classified the last cylinder in the branch as containing needles. If a cylinder, that is, an internode was classified to carry needles, we estimated mass and all-sided area of needles with equations from Lintunen et al. (2011). Segmented and needle-added trees are shown in Fig. 9. We estimated the lower limit of needles (crown base) using an equation from Hynynen et al. (1994). We compared needle masses against ones computed with the aid of biomass equation (Repola et al. 2007) and the correspondence was satisfactory (Supplementary material1).

Finally, the segmented TLS trees were imported into the internal presentation of LIGNUM (see Perttunen et al. 1996). The measured trees could be processed, e.g. in the calculation of the loss function, just as the simulated trees.

LIGNUM MODEL

Growth and senescence

The LIGNUM model has been documented e.g. in publications Perttunen et al. (1996, 1998, 2001) and Sievänen et al. (2008). Here we give a brief summary of its traits relevant to this study. LIGNUM grows trees so that, in one year growth cycle, buds flush and produce a growth units with length L and number of buds at distal end N (Fig. 2). Both L and N are affected by the local conditions in tree crown (e.g. incoming light, branching order). L is also

constrained by the requirement that amount of growth is equal to the available resources (photosynthates) at tree level, represented by the global coefficient λ. *L* and *N* can be expressed in general terms as

$$L = \lambda f_L(local\ conditions) \quad (1)$$

$$N = \lambda f_N(local\ conditions) \quad (2)$$

The function f_N specifies the number of lateral buds, as the apical bud is always created. Any bud, including the apical one, dies if it cannot produce a new shoot in the extension growth. What *local conditions* are depends on the specific formulation applied and will be explained below. The factor λ is a global one and determined during each growth cycle so that the carbon balance holds (Perttunen et al. 1996):

$$W_{new}(\triangle) \square W_{second}(\triangle) \square W_{root}(\triangle) \square P \square M \quad (3)$$

where W_{new}, W_{second} and W_{root} are biomass needed to build new shoots (primary growth), in secondary (thickness) growth and in growth of roots, respectively, and P and M are amounts of photosynthesis and respiration during the growth cycle. Implicit in Eq. 3 is that the amounts of primary, secondary and root growths depend on lengths of new shoots (see Sievänen et al. 2008) and thus on λ.

Part of needles of an internode are shed annually (Perttunen et al. 1996). A branch of any order is considered dead when it has lost all its needles. Dead branches are shed.

Radiation calculations

The time step of LIGNUM is one year; we considered the photosynthetically active radiation during the growing period, 1200 MJm^{-2} on a horizontal surface, a typical value for southern Finland (Stenberg 1996). We took into account radiation coming from different points in the upper hemisphere; we considered the radiation coming from 31 evenly distributed directions (six inclinations, five azimuths and zenith direction) (see Perttunen et al. 2001). We calculated the transparency of path from an internode to each point in the upper hemisphere separately (backward ray casting). We assumed that the radiation distribution of the sky was that of a standard overcast day (Ross 1981). The light transmission in the tree crown was calculated using a voxel space approach with 0.2 m voxel box side length. We tested this against the method of pairwise comparison of shoots (Perttunen et al. 1998) used traditionally in LIGNUM and found similarity of results satisfactory (Supplementary material1).

To speed up simulations we grew only one tree and assumed that it is surrounded by a homogeneous forest that grows in the same pace with the tree (cf. Streit et al. 2016).

The course of stand density used in simulations (Supplementary material1) was taken from measured stands. The transmission of radiation in the surrounding forest was calculated as exp[–0.14 x distance travelled x leaf area density]. The extinction coefficient 0.14 is that of a forest consisting of Scots pine shoots (Stenberg 1996). The absorbed radiation (driving photosynthesis) in an internode from each direction was calculated as incoming radiation x STAR x needle area. STAR is the shoot silhouette to total area ratio (Oker-Blom and Smolander 1988). Total incoming and absorbed radiation at an internode were summed over contributions from all directions.

THE COMPONENTS TESTED

Extension growth of new shoots

The first function (onwards LIGNUM) we tried for the length growth of new shoots is the one that was originally in LIGNUM (Perttunen et al. 1996). It combines the effects of local light (q) and branching order (g)

$$f_L(local\ conditions) = f_q(q) f_g(g) \quad (4)$$

the light effect is accounted for with the aid of relative incoming radiation, q = incoming radiation / (unshaded incoming radiation). Fig. 3 shows typical shapes of functions and the parameterization of their shape as piecewise linear curves and their parameterization.

We tried as the second option the approach by Nikinmaa et al. (2003) that replaces the effect of branching order of Eq. 4 with the strength of pathway from tree base to the shoot (onwards VIGOR). We measured the strength of pathway with vigor index (v) that uses diameters of internodes along the path in the assessment of strength (Nikinmaa et al. 2003). The strength values are relative: the strongest pathway has value 1, the others have values in the range (0, 1]. In this case the local conditions are manifested as

$$f_L(local\ conditions) = \begin{cases} f_q(q) f_v(v), & if\ apical \\ f_a(q) f_q(q) f_v(v), & if\ lateral \end{cases} \quad (5)$$

where v is vigor index of the mother shoot and f_q is the effect of light as in Eq. 4. Lateral shoots are somewhat shorter than apical ones, the effect depends on light conditions mediated by function f_a. Typical functions with parameters used in the optimization are shown in Fig. 4.

As the third alternative, we applied extended Borchert-Honda (onwards EBH) model in the way Palubicki et al. (2009) used it. Borchert and Honda (1984) proposed the model as a mechanism to regulate the extent of branching by controlling the distribution of growth resource to buds. Palubicki et al. (2009) used the amount of light received by the buds to guide the distribution of growth resource. We considered the amount of light intercepted by the shoots, that is, the radiation that drives photosynthetic production in LIGNUM. Evaluation of the EBH operates in two passes, Fig. 5. In the first pass, information about the amount of radiation that reaches the shoots with needles flows basipetally, and its cumulative values are stored within the internodes (Q_1, Q_2, Q_3 and Q in Fig. 5). In the evaluation of path strength leading to growing shoots the strength is divided in a branching point according to radiation values of the shoots. For the internodes in Fig. 5 the strength values are

$$S_1 = \frac{S_0(1-\mu)Q_1}{(1-\mu)Q_1 + \mu Q_2 + (1-\mu)Q_3} \quad S_2 = \frac{S_0 \mu Q_2}{(1-\mu)Q_1 + \mu Q_2 + (1-\mu)Q_3} \quad S_3 = \frac{S_0(1-\mu)Q_3}{(1-\mu)Q_1 + \mu Q_2 + (1-\mu)Q_3} \qquad (6)$$

where the parameter μ controls whether the flow of strength (S_0 in Fig. 5) is biased towards the main axis ($\mu > 0.5$) or biased towards the lateral branch ($\mu < 0.5$). Other number than two lateral branches are treated analogously. The strength values of growing shoots are scaled, the largest value being equal to 1. The effect of local conditions is then directly proportional to the strength values

$$f_L(local\ conditions) \cdot S \quad (7)$$

We allowed that, in the first three branching orders, 1-3, μ attained different values μ_1, μ_2, μ_3, for orders > 3, $\mu = \mu_3$. In the optimization, μ_1, μ_2, and μ_3 were parameters.

Shoot growth in lower parts of crown

Shoot growth is controlled directly or indirectly by light in the above formulations. It was apparent in initial simulations that crown base rose often relatively fast. We implemented, using an *ad hoc* function f_B, a mechanism that boosts (onwards BOOST) shoot growth in lower parts of crown by modifying the shoot length of Eq. 1 as

$$L = \lambda\, f_L(local\ conditions)\ x\ f_B(z) \quad (8)$$

where *z* is relative distance from crown base. Eq. 8 is applied only to side branches and lower order branches (Gravelius order > 2). This function may be thought to mimic e.g. the effect of the red to far-red ratio on shoot growth (cf. Ballaré and Pierik 2017). A typical function f_B is shown in Fig. 6.

Production of buds

The number of lateral buds (Eq. 2) is determined as a function of the needle mass of the mother shoot. We estimated the parameter values of this function in all combinations of components. The total number of buds (cf. Eq. 3) is

$$N = 1 + f_N(W_f) \quad (9)$$

where W_f is needle mass of mother shoot. A typical f_N and the parameters used in optimization are shown in Fig. 7.

Effect of local density in crown

We also tried the alternative in which the local density (needle area density or shoot density) affects the extension growth thus considering the available free growing space (cf. Runions et al. 2007). In the case of length growth we checked whether there was enough free space around the tip of a new shoot (Fig. 8A), henceforth SPACE. If there were shoot(s) closer than a certain distance (R) the new shoot was not created. The length of the new shoot in this case can be expressed as

$$L \square \angle f_L(local\ conditions) \angle_{tip} \quad (10)$$

where χ_{tip} equals 1 or 0 depending on closeness of other shoots to new shoots tip. In this case the radius R of the necessary circular free space around the shoot tip was optimized. As an alternative to the free space approach we modified the number of lateral buds a flushing bud

creates: the needle area density in its perception cone affects the number of new buds (onwards BUDVIEW). The perception cone is determined by its angle of aperture and height (Fig. 8b). In this case the number of buds is equal to

$$N = 1 + f_N(W_f) \times f_c(a_f) \quad (11)$$

where a_f is needle area density in the cone. A typical form of function f_c is shown in Fig. 8b. In addition to parameters p19, …, p21 of the function f_c, also the opening angle of the cone, α, was used in optimization. The height of the cone, was fixed to 0.5 m in the calculations.

COMPARISON OF SIMULATIONS AGAINST THE MEASURED TREES

We evaluated each of the 18 alternative formulations (Supplementary material2) by minimizing with respect to relevant parameter values the loss function that measured the distance between simulated and TLS trees. We measured the distance in terms of tree height (H [m]), total all-sided needle area (A_f [m^2]), needle area density (d_f [m^{-1}]), crown radius (R_c [m]), and relative distribution of internode lengths in different branching orders (ρ_l, unitless). This combination of indices defines a comprehensive metrics for comparison of 3D trees. The value of loss function was sum of height, needle area, needle area density, crown width and internode length distribution terms: L = LH + LA + LAD + CW + BD. They were calculated as squared sums of differences of values from modeled (H_m, A_{fm}, d_{fm}, R_{cm}, ρ_{lm}) and measured (H, A_f , d_f , R_c, ρ_l) trees as follows:

$$LH = w_H \times \sum_{t=8,16,25,33}(H_m(t) - H(t))^2 \quad (12a)$$

$$LA = w_A \times \sum_{t=8,16,25,33}(A_{fm}(t) - A_f(t))^2 \quad (12b)$$

$$LAD = w_{AD} \times \sum_{t=8,16,25,33} \int_{V_c} (d_{fm}(u,t) - d_f(u,t))^2 du \quad (12c)$$

$$CW = w_{CW} \times \sum_{t=8,16,25,33}(R_{cm}(t) - R_c(t))^2 \quad (12d)$$

$$BD = w_{BD} \times \sum_{t=8,16,25,33} \sum_{g=1}^{6}(\rho_{lm}(g,t) - \rho_l(g,t))^2 \quad (12e)$$

where, t is tree age (8, 16, 25 and 33 are ages of measured trees), V_c is crown volume and g is Gravelius order of internode (MacDonald 1983; stem = 1, branch = 2, etc.). The integral in Eq. 12c was evaluated with the aid spatial discretization (voxel space, 0.1 m box size) as a sum, and w_H, w_A, w_{AD}, w_{CW}, and w_{BD} are weights.

We applied three sets of values of the weights. First, we determined the values of them with the aid of initial runs so that each term had approximately equal contribution in the loss function. This was achieved with weight set STANDARD: (w_H, w_A, w_{AD}, w_{CW}, w_{BD}) = (0.05, 0.002, 0.11, 10, 10). We varied the values of weights to study the sensitivity of the results obtained with the STANDARD set. The loss function consists of terms related to tree size (*LH*, *LA* and *LCW*) and crown structure (*LAD* and *BD*). We changed the relative importance of size-related and crown structure variables by factor 3. The weight set SIZE: (w_H, w_A, w_{AD}, w_{CW}, w_{BD}) = (0.15, 0.006, 0.11, 30, 10) increased the importance of *LH*, *LA* and *LW*, and weight set CROWN: (w_H, w_A, w_{AD}, w_{CW}, w_{BD}) = (0.05, 0.002, 0.33, 10, 30) did the same for *LAD* and *BD*.

We carried out the minimization with the GA package for genetic algorithms in R (Scrucca 2013). We ran the minimization until the loss function did not change noticeably any more. It

took normally one to two thousand simulation runs (20 – 40 generations with population size 50). Otherwise we used the standard settings of GA: elitism, crossover probability, and mutation probability were equal to 2, 0.8, and 0.1, respectively. The values of parameters in the minimization were restricted within plausible ranges. The parameters that were not in minimization (the set of basic parameter values of LIGNUM, Fig. 1) had always the same values taken mainly from Sievänen et al. (2008) (Supplementary material1).

We combined the model components from three baskets: shoot elongation (LIGNUM, VIGOR, or EBH), spatial control (no spatial control, SPACE or BUDVIEW) and boost of growth in lower parts of crown (BOOST or no BOOST). We ran altogether 54 minimization runs of the loss function (18 per one set of weight values). The parameters used in each minimization was a subset of all 26 parameters in fitting: p1, …, p21 (Figs 3, 4, 6, 7, 8), μ_1, μ_2, μ_3 (Eq. 6), R (Fig. 8a), and α (Fig. 8b). The parameters used in minimization in each run are shown in Supplementary material2.

RESULTS

All possible combinations of components produced loss function (with weight set STANDARD) values that were not drastically different from each other. The lowest and highest loss function values were 31% apart from the mean value (loss function values are in the Supplementary material2). The lowest value of the loss function was achieved with EBH, BUDVIEW and BOOST combination (Table 1). Visualization of the simulated trees with this combination are shown in Fig. 9. EBH shoot elongation was present in all three best loss

function values (Table 1) whereas LIGNUM and VIGOR resulted in the three lowest values of it. It shows that Extended Borchert-Honda mechanism provides best fit to the data.

Evolution of tree height and needle area varied considerably between the 18 combinations of model components, Fig. 10. All combinations of components tended to produce too low needle areas at age 34 and at age 26 also too small tree heights (Fig. 10). This is probably because the target trees form only a pseudo sequence of trees from a stand: their heights may deviate from shape of height growth in one stand. The optimization of parameter values had in some cases resulted in growth trajectories with low height (Fig. 10). It happened both with LIGNUM and VIGOR shoot elongation and also with enhanced growth in lower crown (BOOST). Low height was linked with high needle area reflecting a trade-off between extension growth and needle area. The growth curves resulting from different combinations of model components show roughly similar shapes. Twists in the needle area curves are probably caused by the simplistic way, in which surrounding stand grows at the same pace with the trees (see *Radiation calculations*): it amplifies small fluctuations.

We take an aggregated approach in the analysis of the component combinations: we compare the mean effect of a component to values of the loss function across all component combinations in Table 2. The measure is difference of the loss function values without and with the component relative to mean loss of all combinations. EBH shoot elongation provides clearly the best fit with almost all measures: it is inferior to LIGNUM or VIGOR only in needle area density. EBH provides clearly much lower values of the loss function in other characteristics, both in the ones related to tree size and crown structure. VIGOR and LIGNUM are quite equal with some variation in parts of the loss function (Eq. 12). VIGOR is better in terms of tree height and succeeds worse with crown width than LIGNUM.

There are some trends in the mean effects of model components for assessing growing space. BUDVIEW is useful or neutral for most of the components of the loss function, only needle area is slightly negatively affected. SPACE is useful only for SIZE and tree height. SPACE enhances length growth improving the fit to height. Both BUDVIEW and SPACE decrease total needle area and they both are not useful for needle area. Overall, BUDVIEW is more useful than SPACE whereas SPACE is useful for tree height only. Promoting shoot growth, independently of radiation conditions at lower parts of the crown (BOOST) seems not to bring benefit to simulations of tree development: it is not useful for any of ALL, SIZE or CROWN. If BOOST is present, tree height does not match observations. BOOST increases allocation of resources to lower part of crown and away from growth of leader shoot. Also crown width is off target; this is because BOOST promotes growing too long branches in the lower crown.

The model components fit together in varying ways. Table 3 shows how the presence of various combinations of SPACE, BUDVIEW or BOOST affects the fit to the data of the shoot elongation formulations. LIGNUM and VIGOR benefit clearly if BUDVIEW is present. Presence of all the other combinations do not improve LIGNUM shoot elongation. VIGOR benefits also from the presence of SPACE and BUDVIEW together with BOOST, all other combinations are detrimental to the fit to the data. EBH in turn seems to benefit from BOOST in all possible combinations. On the other hand, SPACE or BUDVIEW alone do not improve the fit to the data of EBH (Table 3). The lowest values of the loss function with different shoot elongation formulations were achieved in combinations LIGNUM & BUDVIEW (0.0448), VIGOR & SPACE (0.0428), and EBH & BUDVIEW & BOOST (0.0394) showing also that the model components fit together in various way. The lowest values with LIGNUM and

VIGOR shoot extension were 13% and 9% higher than that of EBH. The combinations correspond to the highest values of usefulness in Table 3.

Adjusting parameter values when tree size is important (SIZE set of weights) or crown characteristics are important (CROWN set of weights) changes the usefulnesses slightly (Table 4, loss function values are in the Supplementary material2) but does alter the general picture. The order of usefulnesses for shoot elongation is EBH, VIGOR and LIGNUM with all sets of weights. The usefulness values of shoot elongation model components with SIZE set of weights are quite close to values with STANDARD weights. The usefulness of VIGOR is increased considerably with weight set CROWN whereas that of LIGNUM is much decreased. VIGOR can thus capture the development crown structure relatively well but LIGNUM does not.

The density control (SPACE or BUDVIEW) is not useful at all with SIZE set of weights. For CROWN set of weights, the result is similar to the case STANDARD: BUDVIEW is useful, SPACE is not. It seems thus that the density control is important for capturing the crown development. BOOST is not useful or only marginally useful (with weight set CROWN).

DISCUSSION

This study is an example how segmented TLS data can be readily used in the context of a shoot-based model. This is one step in the process in which improvements in data collection technology, such as TLS, make automatic acquisition of the 3D structures increasingly feasible at various spatial scales for developing FSPMs. When forest scale 3D structural data can be

easily obtained using TLS and the methods to use them in model assessment are developed accordingly, construction and testing of forest FSPMs will be more efficient than before. It was not only the 3D structure (i.e. a collection of woody internode cylinders) of trees that we used but also information about amounts of needles in the internodes. This kind information will be increasingly available from TLS when e.g. analysis of spectral characteristics of the TLS point clouds becomes commonplace (Hakala et al. 2012).

Shoot extension based on the Extended Borchert-Honda (EBH) model worked best within LIGNUM model in this study. Modifying the number of lateral buds a flushing bud creates as a function needle area density (BUDVIEW) turned out to be a useful model component too. This result comes from an aggregated analysis in which we made comparisons across all model component combinations. Promoting shoot growth in lower parts of crown independently of light conditions (BOOST) did not improve the fit to the data with original LIGNUM (LIGNUM) or vigor index (VIGOR) formulations of shoot growth. However, BOOST worked well with EBH. Density control was useful for all shoot extension formulations, BUDVIEW for EBH and LIGNUM and SPACE for VIGOR. The lowest value of the loss function was achieved with the combination EBH, BOOST and BUDVIEW. The best combinations for LIGNUM and VIGOR employed only BUDVIEW or SPACE. This shows that the components fit together in different ways. The lowest loss function values of LIGNUM and VIGOR were around ten percent higher than that of EBH. This indicates that these shoot extension formulations are also able to account for crown dynamics fairly well with suitable set of other model components.

We tested the combinations of model components against the TLS data by minimizing the loss function with respect of relevant parameters in the functions using genetic algorithms. We did

not test whether all parameters in the combinations were identifiable. It is thus possible that the minimum value of the loss function could have been reached with many combinations of values of the parameters. We ran the minimization long enough to make sure that the minimum of the loss function had been achieved. Our aim was to screen between model components on the basis of values of the loss function and we were not particularly interested in values of the parameters (the values of parameters were constrained to reasonable ranges). We therefore deemed this approach satisfactory. As the genetic algorithms are not very prone to stuck in local optima (Scrucca 2013) we trusted that the real minimum of the loss function had indeed been found. Another problem with too many parameters with respect of data can be that the model follows a peculiarity in the data (overfitting). This could be potentially dangerous for our conclusions. However, we summarize results per function (rule of development), not per combination of them, we think that the danger of false conclusions due to overfitting is minor. Further work, for example parameter estimation of a certain combination of rules of development, would warrant using a larger data set and more sophisticated methods of analysing 3D growth models (e.g. Cournède et al 2012).

Our data of four trees is rather small as a sample. However, the data was used to analyse the crown structure of the trees with fine resolution: the TLS data was segmented to branches up to sixth branching order and the amounts of needles they carry was also evaluated. This made it possible to utilize of needle area and crown structure variables as a part of loss function that measures the difference between measured and simulated trees. Due to small number of measured trees, we did not have satisfactory information about the variances and covariances of the variables that were included into the loss function. With this limited prior information at hand we deemed that a linear combination of terms as a loss function is a logical choice. The weights were determined so that each term in the loss function was approximately equally

546 important. We did a simple sensitivity analysis on the basis of two groups of variables in the
547 loss function: those related to tree size and crown structure. It shows that changes in the loss
548 function affects the usefulnesses to some degree but does not alter the main results: the order of
549 usefulnesses for shoot elongation (EBH, VIGOR, LIGNUM), the usefulness of density control
550 by BUDVIEW and no or only marginal usefulness of promoting growth at lower parts of
551 crown (BOOST).
552
553 We made the evaluation for a simplified case, in which one tree was simulated but assuming
554 that it is surrounded by a homogeneous forest. Tree height, height of crown base etc. of the
555 forest was the same with the simulated tree. Density of the forest was the density in which the
556 trees had grown. This simple setting may have had its effect on results but it is difficult to
557 assess its magnitude. Furthermore, the data of comparison has been obtained from trees taken
558 from different forest stands. Even though we tried to make sure that growing conditions (site
559 quality, forest management etc.) of the forests had been as accurately as possible, it is not the
560 same as measuring one tree at different points of time. This is a common problem in forest
561 growth studies (Pretzsch 2009, p. 35). It can be managed by sampling many trees. Due to
562 workload of detailed TLS measurements that are suitable for segmentation done in this study,
563 sampling of many trees was not possible in our case.
564
565 Extended Borchert-Honda model derives shoot growth on the basis of amount of light the
566 shoots along the path from the growing shoot to tree base have intercepted. In a junction, apical
567 and lateral branches (and shoots) are differentiated with a parameter (μ in Eq. 6). Also VIGOR
568 shoot elongation is based on the strength of path from tree base to the shoot but the strength is
569 evaluated with the aid of relative thicknesses of the branches. VIGOR method thus relies on
570 past performance (accumulated growth) in evaluating the path strength whereas EBH method

uses the current condition (light) in assessing the strength. Our results indicate that the growth based on current conditions is more suitable. The original LIGNUM shoot elongation considers only the branching order as the "path strength" factor. It is therefore understandable that it did not stand out. Both VIGOR and LIGNUM methods make use also of the local light conditions (Eqs 3 and 4). The EBH method lumps both effects of light and crown structure along the path to one factor (function) that uses only one parameter – dependent on axis order in our case – that determines relative priorities of apical and lateral directions. It could be that this difference in the effect of light (local vs along a path) caused that promoting shoot growth in the lower parts of crown (BOOST) was useful for EBH but neither for LIGNUM nor VIGOR. Attractive is that EBH employs a low number of parameters, three versus five in LIGNUM and eight in VIGOR. In the best fit case, the values of the EBH parameters were 0.614, 0.615 and 0.517 for branches, side branches and higher order branches, respectively. These values correspond to a rather strong apical preference in the first two orders a lower one in the higher order branches.

We demonstrated how segmented TLS data can be used in the context of a shoot-based model to select model components. We could sort out the importance of the components for the model. Due to the small size of the data as a pseudo growth sequence, applying the distance metric between data and simulations as a simple linear combination and the limited sensitivity analysis, the results need to be regarded as preliminary. The study demonstrates the applicability of TLS data as a phenotyping tool that can readily operate in model evaluation for structural characteristics such as tree height, total needle area, spatial distribution of needle area, crown width, and shoot lengths of different branching orders at different tree age.

LITERATURE CITED

Ballaré, C L, Pierik, R. 2017. The shade-avoidance syndrome: multiple signals and ecological consequences. Plant, Cell & Environment, doi: 10.1111/pce.12914.

Beyer R, Letort V, Bayer D, Pretzsch H, Cournède P-H. 2017a Leaf density-based modelling of phototropic crown dynamics and long-term predictive application to european beech. *Ecological Modelling* 347:63 – 71.

Beyer R, Letort V, Bayer D, Pretzsch H, Cournède P-H. 2017b. Validation of a functional-structural tree model using terrestrial lidar data. *Ecological Modelling* 357: 55 – 57.

Borchert, R., Honda, H., 1984. Control of decvelopment in the bifurcating branch system of tabebuia rosea: A computer simulation. Botanical Gazette 145 (2), 184-195.

Cajander A K. 1949. Forest types and their significance. Acta For Fenn 56:1–69.

Calders K, Newnham G, Burt A, Murphy S, Raumonen P, Herold M, Culvenor D, Avitabile V, Disney M, Armston J, Kaasalainen M. Non-destructive estimates of above-ground biomass using terrestrial laser scanning. Methods in Ecology and Evolution, Vol. 6, No. 2, pp. 198-208.

Costes E, Smith C, Renton M, Guédon Y, Prusinkiewicz P, Godin C. 2008. MAppleT: simulation of apple tree development using mixed stochastic and biomechanical models. Functional Plant Biology 35: 936–950.

Cournède, P.-H., Mathieu, A., Houllier, F., Barthèlèmy, D., de Reffye, P., 2008. Computing competition for light in the Greenlab model of plant growth: A contribution to the study

620 of the effects of density on resource acquisition and architectural development. Annals
621 of Botany 101, 1207–1219.
622
623 Cournède P-H, Chen Y, Wu Q, Baey C, Bayol B. 2012. Development and Evaluation of Plant
624 Growth Models: Methodology and Implementation in the PYGMALION Platform.
625 Math. Model. Nat. Phenom. 7(2): 32–48, 2012.
626
627 Da Silva D, Qin L, DeBuse C, DeJong TM. 2014. Measuring and modelling seasonal patterns
628 of carbohydrate storage and mobilization in the trunks and root crowns of peach trees.
629 Annals of Botany 114: 643–652.
630
631 Ford E D, Sorrensen KA. 1992 Theory and models of inter-plant competition as a spatial
632 process. In: Individual-based models and approaches in ecology, DeAngelis DL, Gross,
633 LJ (editors), pp. 363-407, Routledge, Chapman & Hall, New York, ISBN 0-412-03161-
634 2.
635 Franco, M. 1986. The influence of neighbours on the growth of modular organisms with an
636 example of trees. *Phil. Trans. R. Soc. B* 313: 209-225.
637
638 Gatziolis D, Lienard J F, Vogs, A, Strigul, N S. 2015. 3d tree dimensionality assessment using
639 photogrammetry and small unmanned aerial vehicles. *PLoS ONE* 10 (9): 1–21.
640
641 Godin C, Sinoquet H. 2005. Functional-structural plant modelling. *New Phytologist*
642 **166**(3):705-708.
643

644 Hakala T, Suomalainen J, Kaasalainen S, Chen Y. 2012. Full waveform hyperspectral LiDAR
645 for terrestrial laser scanning. Optics Express 20: 7119–7127.
646
647 Host G E, Stech H W, Lenz K E, Roskoski K, Mather R. 2008. Forest patch modeling: using
648 high performance computing to simulate aboveground interactions among individual
649 trees. Functional Plant Biology 35(9/10): 976-987l
650
651 Hynynen J, Ojansuu R, Hökkä H, Siipilehto J, Salminen H, Haapala P. 2002. Models for
652 predicting stand development in MELA System. *Metsäntutkimuslaitoksen tiedonantoja*
653 835. 116 p.
654
655 Letort V, Cournède P-H, Mathieu A, de Reffye P, Constant T. 2009. Parametric identification
656 of a functional-structural tree growth model and application to beech trees (*Fagus*
657 *Sylvatica*). Functional Plant Biology 35(9/10): 951-963.
658
659 Lintunen, A., Kaitaniemi, P., Sievänen, R., Perttunen, J., 2011. Models of 3d crown structure
660 for scots pine (Pinus Sylvestris L) and silver birch (betula pendula) grown in mixed
661 forest. Canadian Journal of Forest Research 41: 1779-1794.
662
663 MacDonald, N, 1983. Trees and networks in biological models. John Wiley & Sons: Avon.
664
665 Nikinmaa E, Messier C, Sievänen R, Perttunen J, Lehtonen M. 2003. Shoot growth and crown
666 development: effect of crown position in three-dimensional simulations. Tree
667 Physiology 23: 129-136.
668

669 Oker-Blom P, Smolander, H. 1988. The ratio of shoot silhouette area to total needle area in
670 Scots pine. Forest Science 34 (4): 894–906.
671
672 Palubicki W. 2013. A computational study of tree architecture. Ph.D. thesis, Department of
673 Computer Science, University of Calgary, 2500 University Dr. NW Calgary, Alberta, Canada
674 T2N 1N4.
675
676 Palubicki W, Horel K, Longay S, Runions A, Lane B, Mech R, Prusinkiewicz P. 2009. Self-
677 organizing tree models for image synthesis. ACM Transactions on Graphics 28(3): 58:
678 1-10.
679
680 Perttunen, J., Sievänen, R., Nikinmaa, R., Salminen, H., Saarenmaa, H. and Väkevä, J. 1996.
681 LIGNUM: a tree model based on simple structural units. Annals of Botany 77:87-98.
682
683 Perttunen, J., Sievänen R., Nikinmaa, E. 1998. LIGNUM: A Model Combining the Structure
684 and the Functioning of Trees. Ecological Modelling 108:189-198.
685
686 I. Potapov, M. Järvenpää, M. ̊Akerblom, P. Raumonen, and M. Kaasalainen. Data-based
687 stochastic modeling of tree growth and structure formation, 2016.
688
689 Pretzsch H. 2009. Forest dynamics, growth and yield. Springer, Berlin / Heidelberg.
690
691 Raumonen, P, Kaasalainen, M, Åkerblom, M, Kaasalainen, S, Kaartinen, H, Vastaranta, M,
692 Holopainen, M, Disney, M, Lewis, P. 2013. Fast automatic precision tree models from
693 terrestrial laser scanner data. Remote Sensing 5 (2): 491–520.

URL http://www.mdpi.com/2072-4292/5/2/491

Repola J, Ojansuu R, Kukkola M. 2007. Biomass functions for scots pine, norway spruce and birch in Finland. Working Papers of the Finnish Forest Research Institute 53, Finnish Forest Research Institute.

Ross J. 1981. The radiation regime and architecture of plant stands. Dr W. Junk Publishers: The Hague, The Netherlands.

Runions A, Lane B, Prusinkiewicz P. 2007. Modeling trees with a space colonization algorithm. In: Ebert, D., M_erillou, S. (Eds.), Eurographics Workshop on Natural Phenomena. pp. 63-70.

Scrucca L. 2013. GA: A package for genetic algorithms in R. Journal of Statistical Software 53 (4): 1-37. URL http://www.jstatsoft.org/v53/i04/

Sievänen R, Perttunen J, Nikinmaa E, Kaitaniemi P. 2008. Toward extension of a single tree functional structural model of Scots pine to stand level: effect of the canopy of randomly distributed, identical trees on development of tree structure. Functional Plant Biology 35(9/10): 964-975.

Streit K, Henke M, Bayol B., Cournède P H, Sievänen R., Kurth W. 2017. Impact of geometrical traits on light interception in conifers: Analysis using an FSPM for Scots pine. In: Proceedings 2016 IEEE International Conference on Functional-Structural

718 Plant Growth Modeling, Simulation, Visualization and Applications (FSPMA 2016), 7-
719 11 Nov. 2016, Qingdao (China), IEEE Press, Beijing 2016, 194-203.
720
721 Stenberg P. 1996. Metsikön rakenne, säteilyolot ja tuotos. University of Helsinki, Department
722 of Forest Ecology Publications no. 15. [in Finnish].
723
724 Sterck F, Schieving, F. 2007. 3-D growth patterns of trees: Effects of carbon economy,
725 meristem activity, and selection. Ecological Monographs 77: 405-420.
726
727 Takenaka A. 1994 A simulation model of tree architecture development based on growth
728 response to local light environment *Journal of Plant Research* 107, 321-330.
729
730 Wang F, Letort V, Lu Q, Bai X, Guo Y, de Reffye, P, Li B. 2012. A functional and
731 structural Mongolian Scots Pine (Pinus Sylvestris var. mongolica) model integrating
732 architecture, biomass and effects of precipitation. PLOS ONE 7 (8):1-13.
733
734
735
736 FIGURE CAPTIONS
737
738 Figure 1. Principle of testing of different combinations of model components. The
739 minimization of the loss function (Eq. 12) revealed how well the combination of the
740 components fits the data. It was defined as a linear combination of squared error terms between
741 simulated trees and those segmented from TLS data (Eq. 12). On the right side, it is shown as
742 an example how the functions of shoot elongation of the original LIGNUM formulation

743 (Perttunen et al. 1996) (Fig. 2) were parameterized (as piecewise linear curves) for
744 minimization: parameters p1, …, p5. Other functions were parameterized in a similar manner.
745
746 Figure 2. The principle of growth in LIGNUM model: a bud (at the end of a shoot) produces a
747 new growth unit consisting of a shoot with length L and three buds (apical one and two lateral
748 ones) during one growth cycle.
749
750 Figure 3. Typical shapes of functions f_q (left panel) and f_g (right panel) of Eq. 4 controlling
751 shoot length in the formulation according to Perttunen et al. (1996). q is relative incoming
752 radiation = incoming radiation / (unshaded value), g is Gravelius order of the mother shoot
753 (MacDonald 1983; stem = 1, branch = 2, etc.). Shown are the parameters p1, …, p5 that
754 control the shape of the functions and were used in the optimization.
755
756 Figure 4. Typical vigor index (f_v) and apical (f_a) functions. v is vigor index (Nikinmaa et al.
757 2003) and q is relative incoming radiation = incoming radiation / (unshaded value). Indicated
758 are the parameters p6, …, p11 that were used in the optimization.
759
760 Figure 5. The principle of EBH calculation. The intercepted radiation (Q values) are first
761 accumulated basipetally, thus $Q = Q_1 + Q_2 + Q_3$. The strength values (S) flow acropetally
762 according to Eq. 6.
763
764 Figure 6. A typical shape of function f_B of Eq. 8. It is determined by parameters p12, p13, and
765 p14 that were used in the optimization.
766

767 Figure 7. A typical function f_N (W_f) for number of lateral buds as a function of needle mass of
768 mother shoot, W_f. Shown are also parameters p15, …, p18 that determine its shape and were
769 used in the optimization.
770
771 Figure 8. A: Requirement of free growing space of radius R around the tip of a new shoot: this
772 one cannot grow (χ_{tip} = 0) since other shoot is inside the growing space, B: Evaluation of
773 needle area density in a cone with α/2 half angle with maximum distance D, and C: a typical
774 function reducing the number of lateral buds (Eq. 11) as a function needle area density in the
775 cone of perception of a bud (c). D was fixed to 0.5 m the optimizations.
776
777 Figure 9. Scanned (left) and best fit trees (right) (combination EBH & BUDVIEW & BOOST)
778 at ages 8, 16, 25 and 33 years, heights are those of the scanned trees.
779
780 Figure 10. A: Tree heights (solid lines) and heights of crown base (dashed lines) of best fit runs
781 of all component combinations versus values of target trees (lines with circles). B: The same
782 for needle area. Red (LIGNUM & BOOST), blue (VIGOR & BOOST), green (VIGOR &
783 SPACE & BOOST) and cyan (VIGOR & BUDVIEW) colors mark runs that have distinctively
784 different evolutions of height or needle area in comparison to the rest of runs.
785

Table 1. The combinations that produce three lowest and highest values of the loss function with weight set STANDARD: (w_H, w_A, w_{AD}, w_{CW}, w_{BD}) = (0.05, 0.002, 0.11, 10, 10).

	Three lowest values			Three highest values		
Loss function value	0.0394	0.0396	0.0427	0.0572	0.0647	0.0703
Combination	EBH BUDVIEW BOOST	EBH BOOST	EBH SPACE BOOST	VIGOR BOOST	LIGNUM BOOST	VIGOR SPACE BOOST

Table 2. Usefulness[1] of model components in percent values for the combined loss function (ALL), combination of terms related to tree size (SIZE) and crown characteristics (CROWN) as well as for all components of Eq. 12. Positive values mean that loss function values are smaller on average when the component is in use and negative values the opposite. LIGNUM, VIGOR, EBH and BOOST affect shoot elongation and SPACE and BOOST affect growth through local density. Weight set STANDARD was used in the loss function ((w_H, w_A, w_{AD}, w_{CW}, w_{BD}) = (0.05, 0.002, 0.11, 10, 10))

	Shoot elongation			Density control		Growth of lower crown
	LIGNUM	VIGOR	EBH	SPACE	BUDVIEW	BOOST
ALL[2]	-12	-7	19	-6	11	-7
SIZE[3]	-22	-11	33	9	5	-11

CROWN[4]	-9	-5	14	-11	12	-6
LH	-66	-34	99	61	20	-40
LA	-1	0	1	-16	-2	2
LAD	9	10	-19	10	1	1
CW	-3	-78	81	-54	24	-62
BD	-54	7	47	-30	29	13

[1]Defined as (mean loss without component – mean loss with component) / mean loss of all combinations

[2]ALL = LH + LA + LAD + CW + BD (Eq. 12)

[3]SIZE = LH + LA (Eq. 12)

[4]CROWN = LAD + CW + BD (Eq. 12)

Table 3. Usefulness[1] of combinations of SPACE, BUDVIEW and BOOST in per cent values in conjunction with shoot elongation formulations LIGNUM, VIGOR and EBH. Note that usefulness is defined here other way than in Table 2. Weight set STANDARD was used in the loss function ((w_H, w_A, w_{AD}, w_{CW}, w_{BD}) = (0.05, 0.002, 0.11, 10, 10)).

Combination	LIGNUM	VIGOR	EBH
SPACE	-20	21	-15
BUDVIEW	19	17	-11
BOOST	-20	-7	8
SPACE & BOOST	-1	-33	2
BUDVIEW & BOOST	-2	9	8

[1]Defined as (loss with LIGNUM, VIGOR or EBH only - loss with combination) / mean loss of all combinations

Table 4. Usefulness of model components in percent values for the combined loss function (ALL = LH + LA + LAD + BD + CW) with weight sets SIZE and CROWN. See Table 2 for explanation of symbols.

	Shoot elongation			Density control		Growth of lower crown
	LIGNUM	VIGOR	EBH	SPACE	BUDVIEW	BOOST
	Weight set SIZE: (w_H, w_A, w_{AD}, w_{CW}, w_{BD}) = (0.15, 0.006, 0.11, 30, 10)					
ALL	-14	-7	21	-1	-1	-24
	Weight set CROWN: (w_H, w_A, w_{AD}, w_{CW}, w_{BD}) = (0.05, 0.002, 0.33, 10, 30)					
ALL	-32	13	19	-17	12	2

SUPPLEMENTARY MATERIAL

File1: Supplementary material1

Comparison of foliage mass to biomass equation

The main parameter values applied in the simulations

Comparison of voxel-based and pairwise light calculation

Stand density in simulations

File2: Supplementary material2

Table 1. Summary of tested model components and parameters in the optimization

Table 2. Values of loss function (TOTAL) and its components in the minimization runs. STANDARD set of weights

Table 3. Values of loss function (TOTAL) and its components in the minimization runs. SIZE set of weights

Table 4. Values of loss function (TOTAL) and its components in the minimization runs. CROWN set of weights

LIGNUM
Unmodified with basic parameter values

Parameters in tested model components

Modified LIGNUM, parameters only of tested model components in estimation:
p1, …, pn

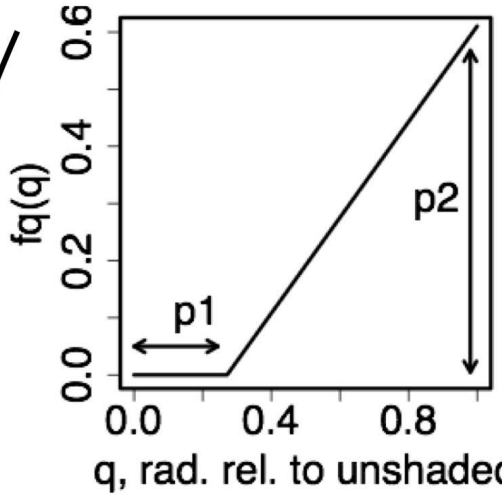

Example

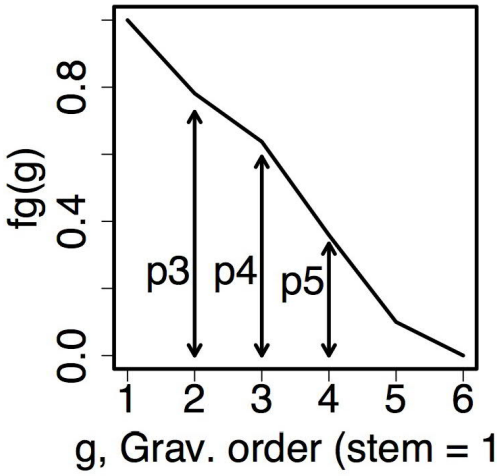

functions

TLS Data

Genetic algorithm: minimization of loss function using
p1, …, pn

Other parameters, functions …

Result: loss function value with best fit parameter values
= how well these components work,
altogether 18 combinations of components tested

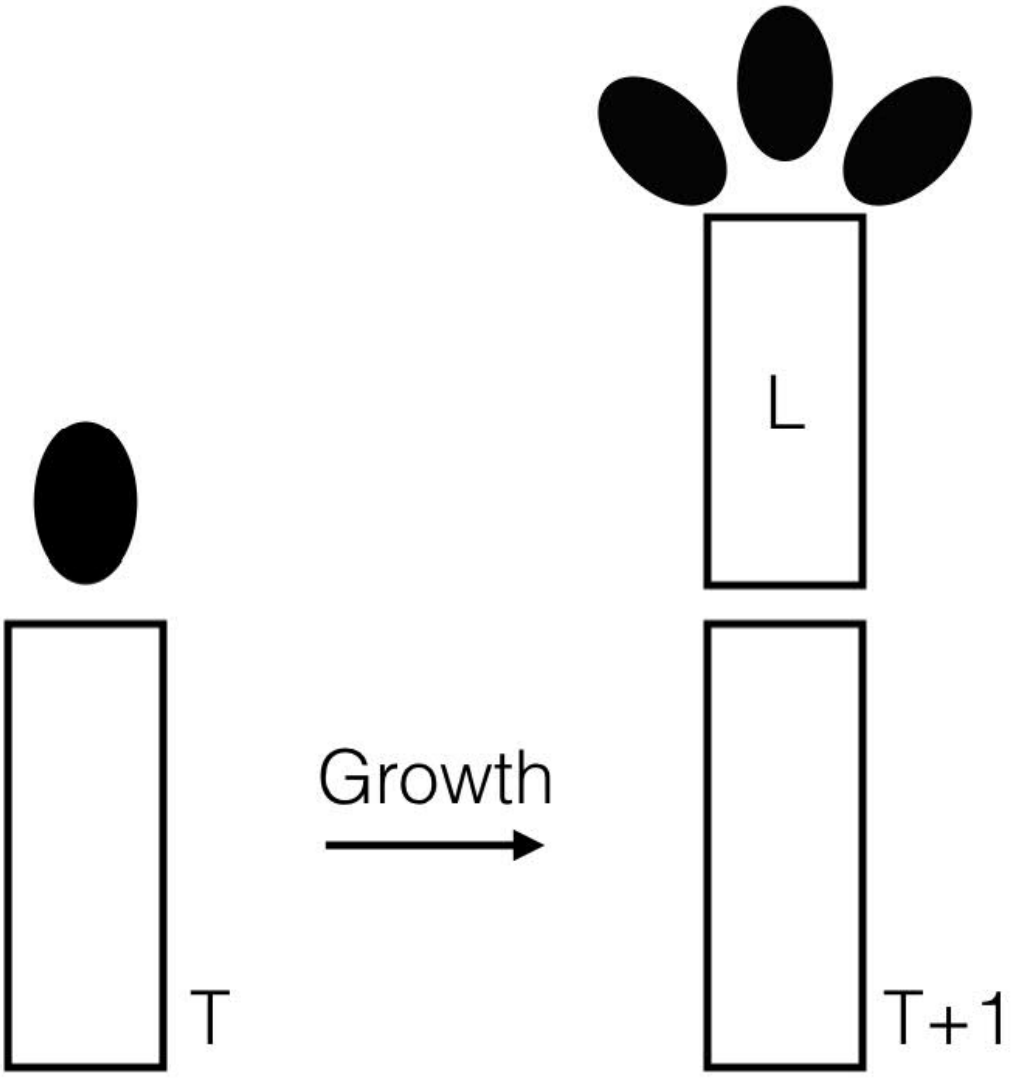
L
Growth
T
T+1

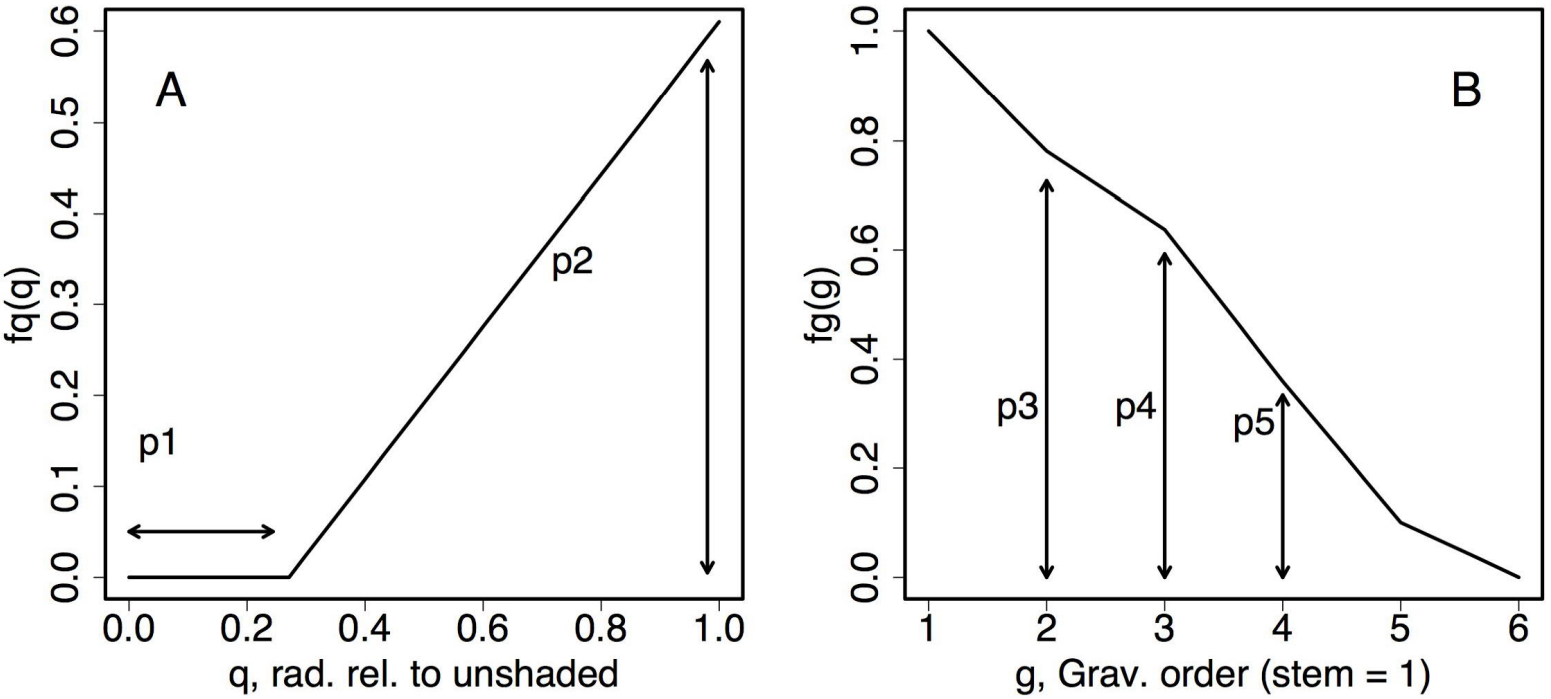
A
B
fq(q)
fg(g)
q, rad. rel. to unshaded
g, Grav. order (stem = 1)
p1
p2
p3
p4
p5
0.0
0.1
0.2
0.3
0.4
0.5
0.6
0.8
1.0
1
2
3
4
5
6

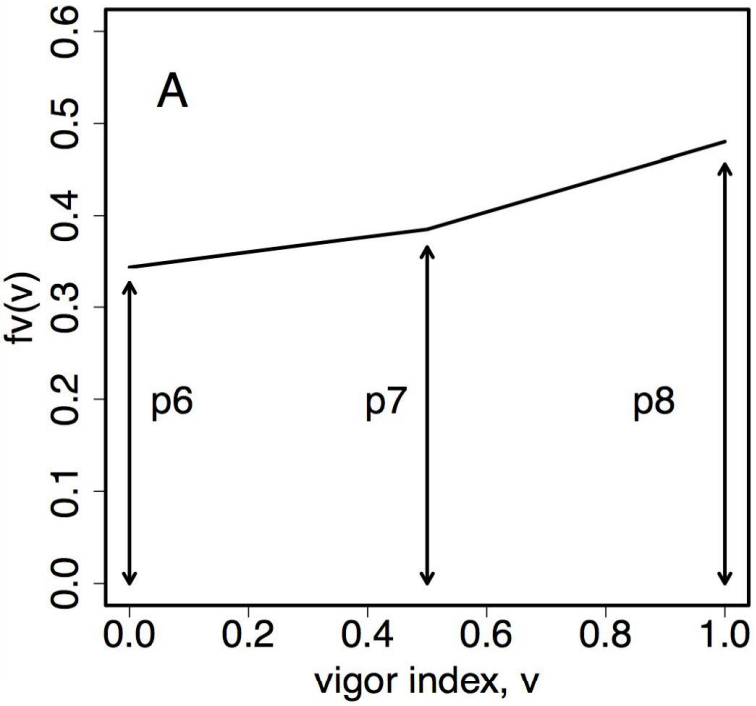
A
fv(v)
0.0
0.1
0.2
0.3
0.4
0.5
0.6
p6
p7
p8
0.0
0.2
0.4
0.6
0.8
1.0
vigor index, v

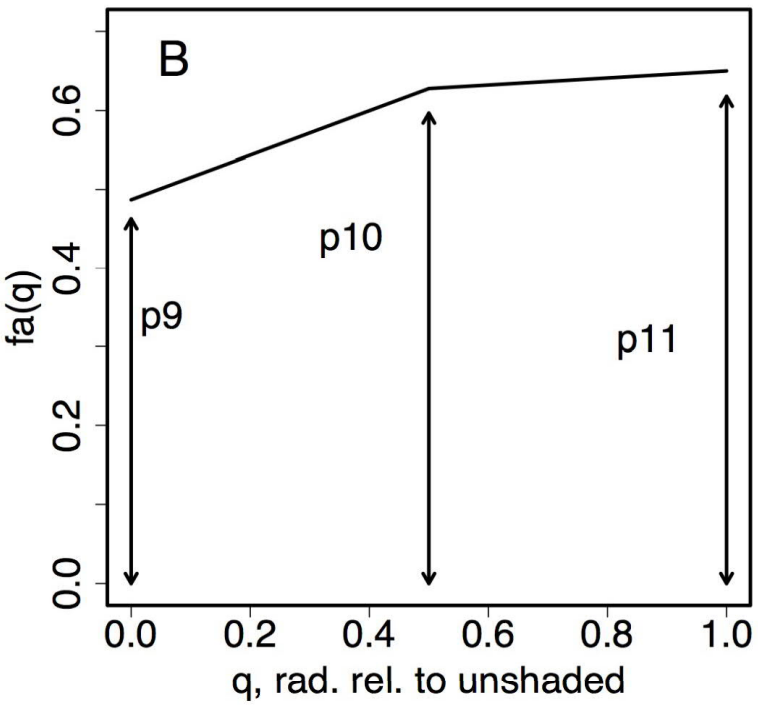
B
fa(q)
0.0
0.2
0.4
0.6
p9
p10
p11
0.0
0.2
0.4
0.6
0.8
1.0
q, rad. rel. to unshaded

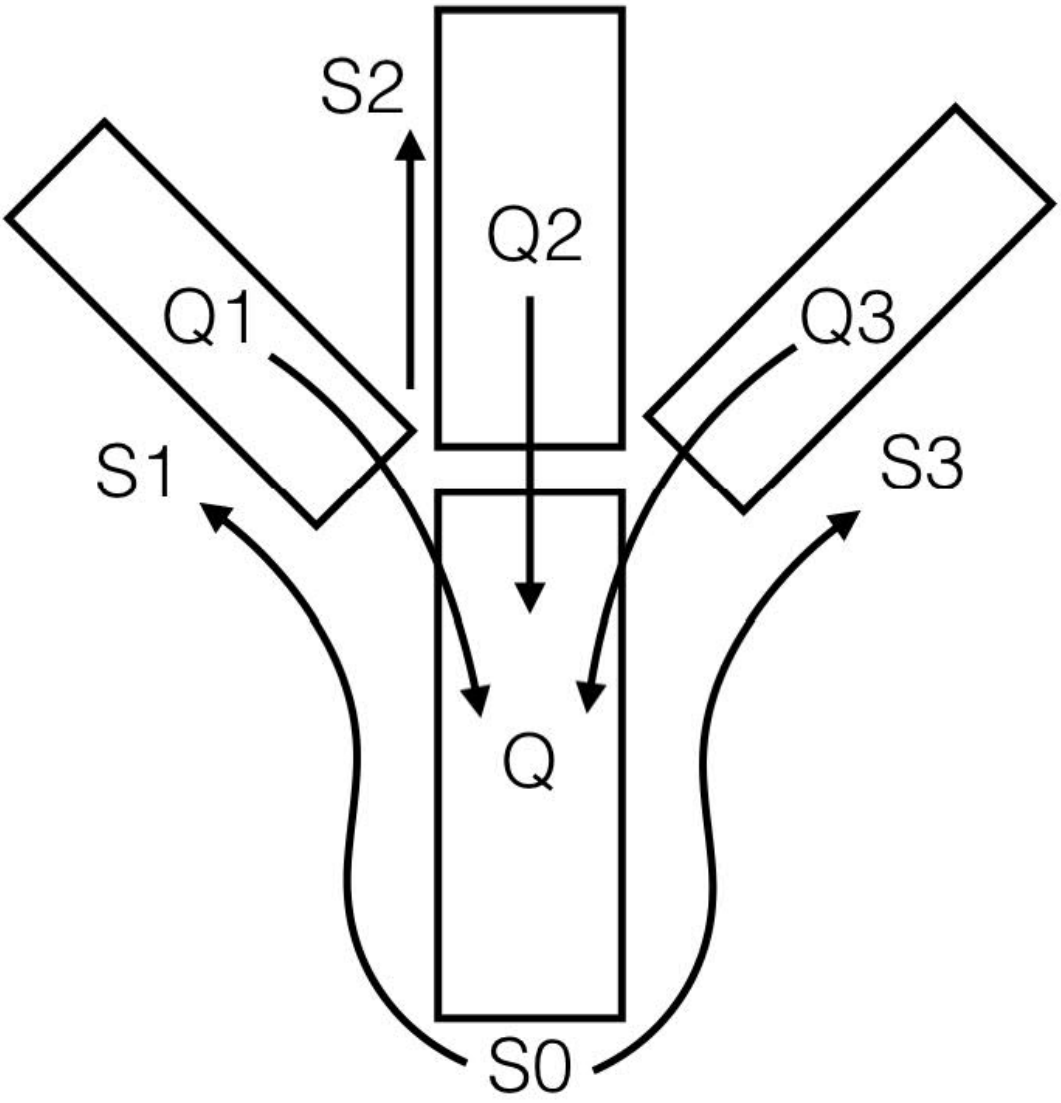
S2
Q2
Q1
Q3
S1
S3
Q
S0

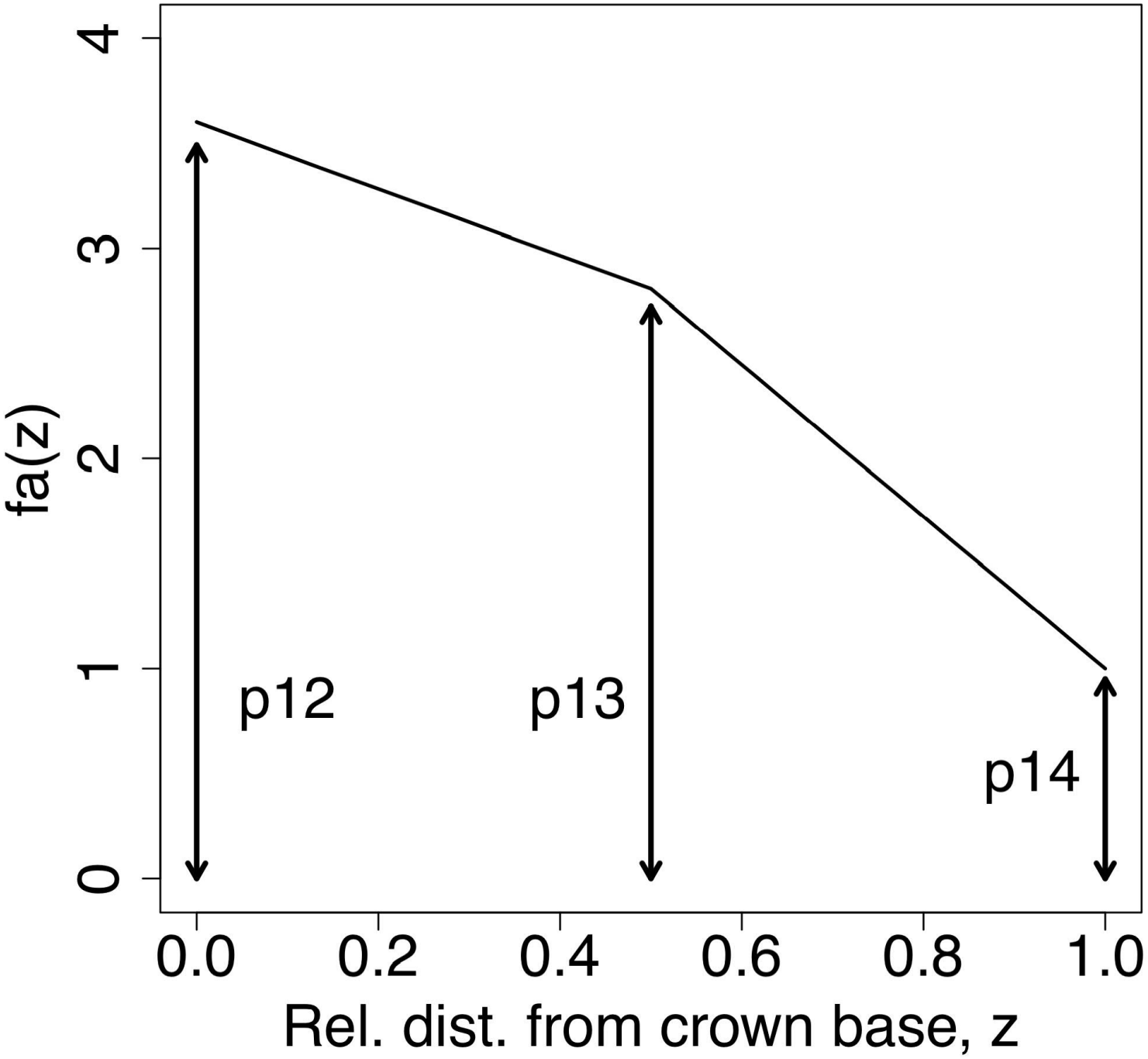
fa(z)
0
1
2
3
4
p12
p13
p14
0.0
0.2
0.4
0.6
0.8
1.0
Rel. dist. from crown base, z

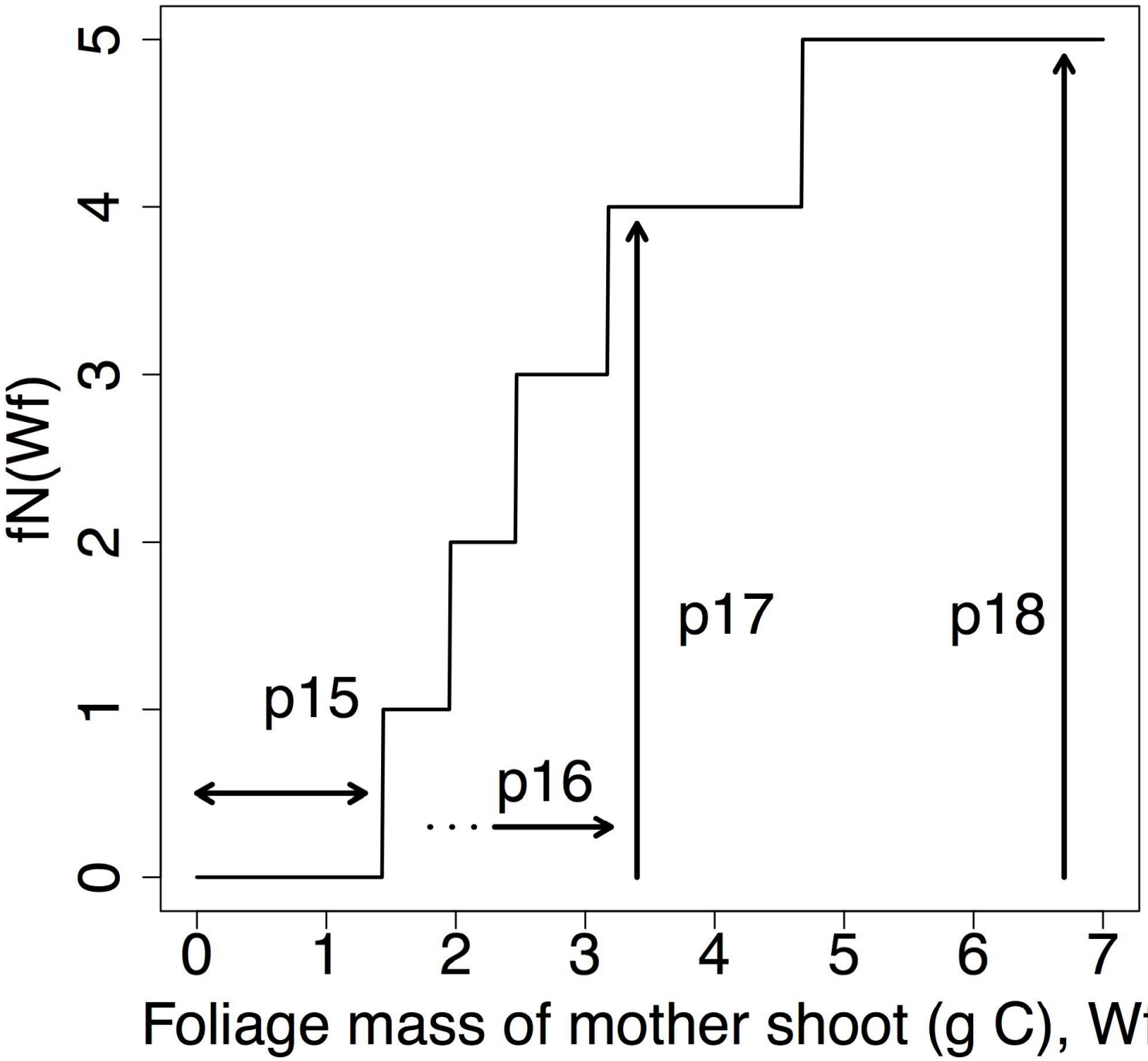
fN(Wf)
0
1
2
3
4
5
p15
p16
p17
p18
0
1
2
3
4
5
6
7
Foliage mass of mother shoot (g C), Wf

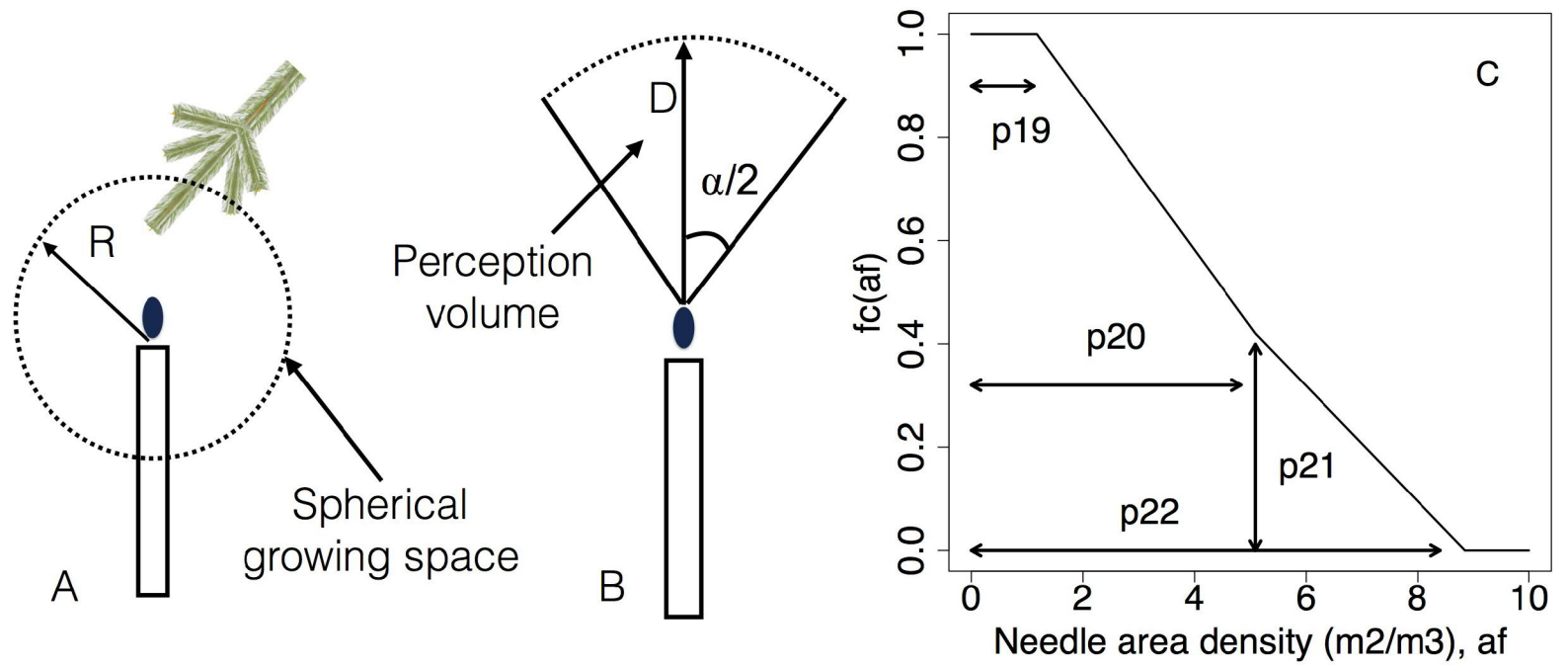
R
Spherical
growing space
A
D
α/2
Perception
volume
B
C
p19
p20
p21
p22
fc(af)
0.0
0.2
0.4
0.6
0.8
1.0
0
2
4
6
8
10
Needle area density (m2/m3), af


8 yrs
H = 2.6 m
16 yrs
H = 7.2 m
25 yrs
H = 12.0 m
33 yrs
H = 13.6 m

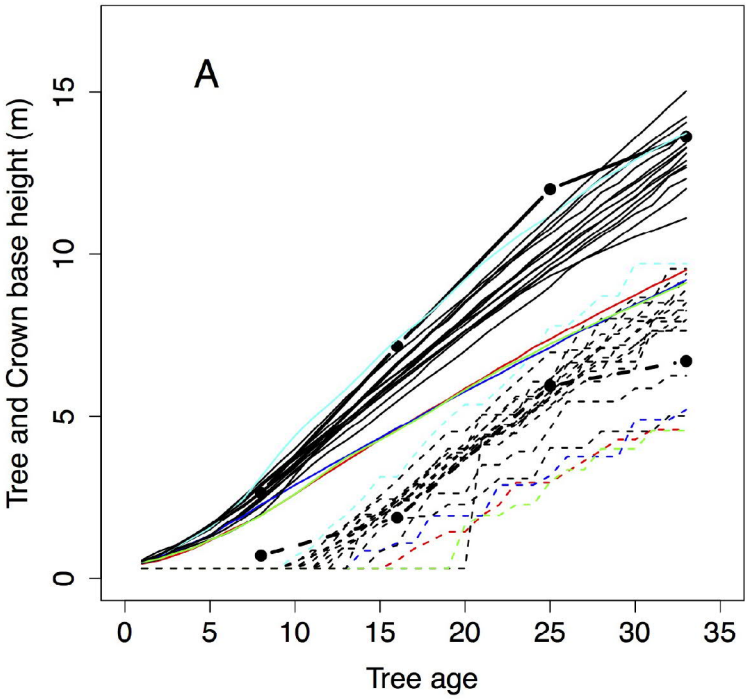
A
Tree and Crown base height (m)
0
5
10
15
0
5
10
15
20
25
30
35
Tree age

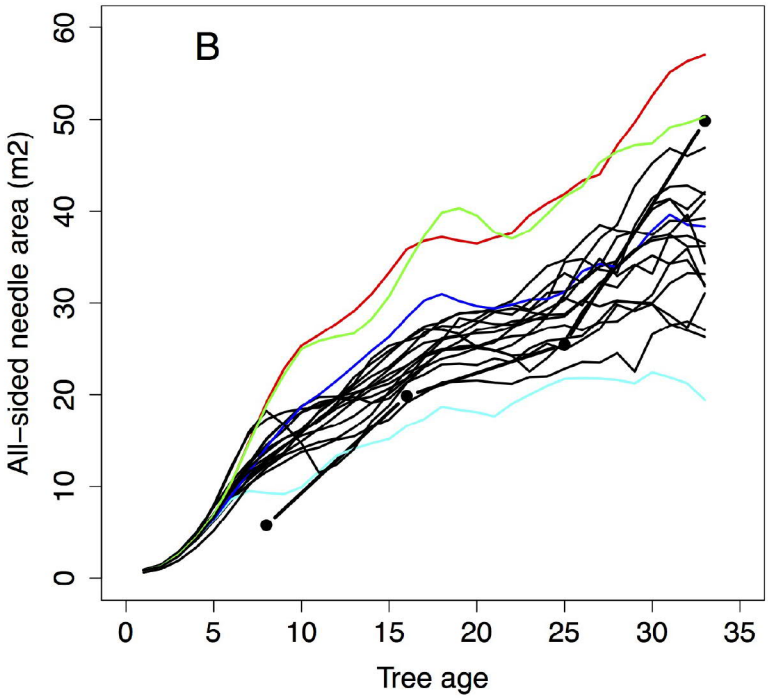
B
All−sided needle area (m2)
0
10
20
30
40
50
60
0
5
10
15
20
25
30
35
Tree age